JOURNAL OF MATERIALS SCIENCE 28 (1993) 4850–4854

Phase formation in drop-tube processing from undercooled $Pd_{77.5}Au_6Si_{16.5}$ melt

MAO ZI-LI, LI CHAO-RONG, CHEN HONG, SHAO XIU-YU
Institute of Physics, Academia sinica, Beijing 100080, People's Republic of China
WANG WEN-KUI
Institute of Physics, Academia sinica, Beijing 100080, International Centre for materials physics, Academia sinica, Shenyang 110015, People's Republic of China

The $Pd_{77.5}Au_6Si_{16.5}$ alloy was studied by drop-tube processing. Palladium solid-solution phase was found in smaller droplets (diameter $D < 400\,\mu m$), while in larger droplets, the intermetallic compound Pd_3Si was observed. The difference in free energy between the undercooled liquid and the solid state, the activation energy for the formation of post-critical nuclei, the nucleation frequency and the crystal growth velocity, were calculated as functions of temperature for palladium solid solution and Pd_3Si phases. These calculations led to time–temperature–transformation curves which were capable of describing the experimental findings on the kinetics of solidification of this alloy.

1. Introduction

The undercooling phenomenon is an important means of preparing metastable, crystalline, as well as amorphous, alloys. The degree of undercooling attainable is controlled by different nucleation processes occurring within the undercooled melt. Nucleation plays an important role in many processes involving phase changes.

In drop-tube processing of alloys, the melt was released at the top of the tube as droplets and solidified as they fell. In a vacuum the droplets solidify under zero gravity, so drop-tube studies may be a useful and cost-effective precursor to research on materials processing in space [1]. On the other hand, high melt undercooling may be achieved in the droplets because of the absence of a container which could catalyse crystal nucleation. In solidification at high undercooling of an alloy, structures far from equilibrium, such as extended solid solutions, metastable compound phases and glasses, may be obtained.

The alloy studied in the present work was $Pd_{77.5}Au_6Si_{16.5}$. The glassy alloy was prepared by a squeeze quenching technique given previously [2], but the microstructure formed in the drop-tube processing has yet not been reported. Other aspects of undercooling and crystal nucleation of the $Pd_{77.5}Cu_6Si_{16.5}$ have been studied widely by directional solidification and containerless solidification [3, 4]. Here we used the element gold instead of copper, the objectives being to see whether the third component (such as gold, copper, etc.) influences the resulting structures of Pd–Si-based alloys in drop-tube processing, whether any new microstructure can be obtained and to try to describe the experimental results quantitatively on the basis of classic nucleation theory. The samples were investigated by X-ray diffraction, scanning electron microscope (SEM) and X-ray energy dispersive spectrum (EDS) analysis. It was shown that depending on the size of droplets, different nucleation processes may occur and different microstructure was obtained.

2. Experimental procedure

The $Pd_{77.5}Au_6Si_{16.5}$ alloy was prepared from pure palladium (99.9 %), gold (99.99 %), and silicon (99.999 %). Weighed components were melted in an arc furnace under argon. A drop tube, 20 m high, was used in our experiment. After the drop tube was evacuated to a pressure below 10^{-7} torr (1 torr = 133.322 Pa), it was refilled with purified dry argon at a pressure of 300 torr in order to increase the cooling rate. Samples of about 0.5 g were remelted in a quartz crucible and dispersed as droplets into the drop tube. Droplets up to 1500 μm diameter solidified during free-fall and were collected at the bottom of the drop tube. Phase composition and the microstructure of the droplets with different sizes were investigated by X-ray diffraction, SEM and EDS analysis.

3. Results

The X-ray diffraction pattern of droplets with different sizes is shown in Fig. 1. Droplets with a diameter of smaller than 400 μm exhibit the diffraction peaks of f c c structure overlapped on an amorphous halo. The lattice parameter of the f c c phase is 0.392 nm, slightly larger than the lattice parameter (3.89 nm) of pure palladium. EDS analysis showed no detectable difference in composition between the amorphous phase and the f c c phase; Au 4 at % and Si 18 at % were present in the f c c phase, so the f c c crystalline phase was identified as a palladium solid-solution.

0022–2461

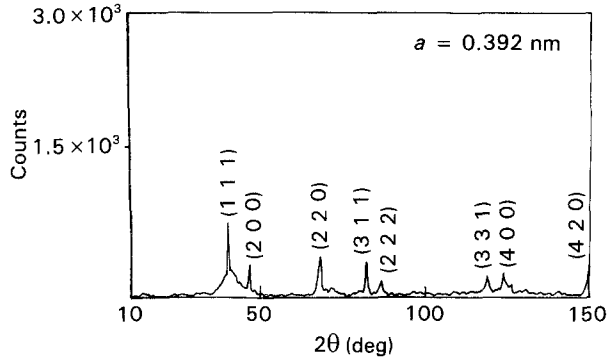

Figure 1 X-ray diffraction pattern of smaller $Pd_{77.5}Au_6Si_{16.5}$ droplets ($D < 400$ μm).

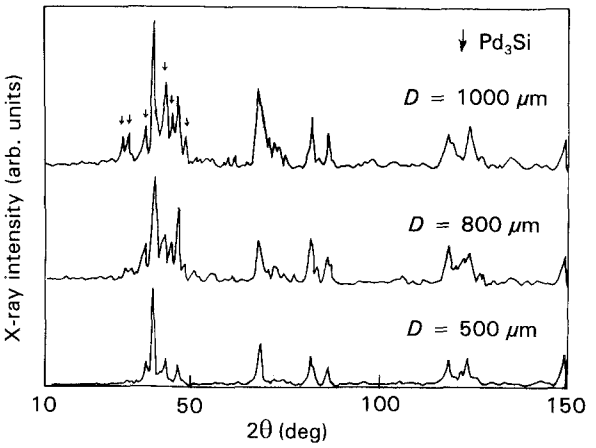

Figure 2 X-ray diffraction pattern of larger $Pd_{77.5}Au_6Si_{16.5}$ droplets ($D > 400$ μm).

For larger droplets ($D > 400$ μm), the new diffraction peaks appear around diffraction angles $\Theta = 31.49°$, 32.583°, 37.243°, 42.262°, 44.054°, and 47.459°, etc. The intensities of the peaks increase as the diameter of the droplets increases, as shown in Fig. 2. The diffraction peaks were indexed in terms of the Pd_3Si phase. By comparison with the resulting structure of $Pd_{77.5}Cu_6Si_{16.5}$ obtained in the drop tube, for both alloys, Pd_3Si intermetallic phase was found to always exist in larger droplets [4], but the palladium solid-solution phase was only present in smaller $Pd_{77.5}$ Au_6 $Si_{16.5}$ droplets.

Fig. 3 shows a scanning electron micrograph of droplets with $D < 400$ μm. The palladium solid-solution phase is seen to be dispersed as fine particles ($D = 0.5$ μm) in a matrix of amorphous phase. In larger diameter droplets, only a lower degree of undercooling is achieved and a significant temperature gradient can be established within the larger droplets before solidification begins. The surface of the droplet cools quicker than the centre, hence a higher undercooling is present in the surface region and a lower one in the centre, thus palladium solid-solution phase is preferentially formed near the surface and Pd_3Si phase nucleates in the centre. This is shown in Figs 4 and 5. As illustrated in Fig. 4, near the surface of the droplet the primary palladium solid-solution grew into unbranched, blocky "blades", whereas Pd_3Si phase was present in the centre of the droplet as dendritic growth, shown in Fig. 5.

The X-ray analysis and electron microscope observation illustrated that the microstructures of the droplets depend on the diameter of the droplets. We expect smaller droplets to achieve, on average, deeper undercooling, because the increased quench rate lowers the onset temperature for nucleation, and heterogeneous nuclei in the melt will be more thinly dispersed in finer droplets. Using the method given by Bayuzick [5], we can estimate the cooling rate of different droplets in the drop tube. The calculated results were $T = 1.5 \times 10^3$ K s^{-1} for $D = 0.18$ mm and $T = 4 \times 10^2$ K s^{-1} for $D = 0.4$ mm.

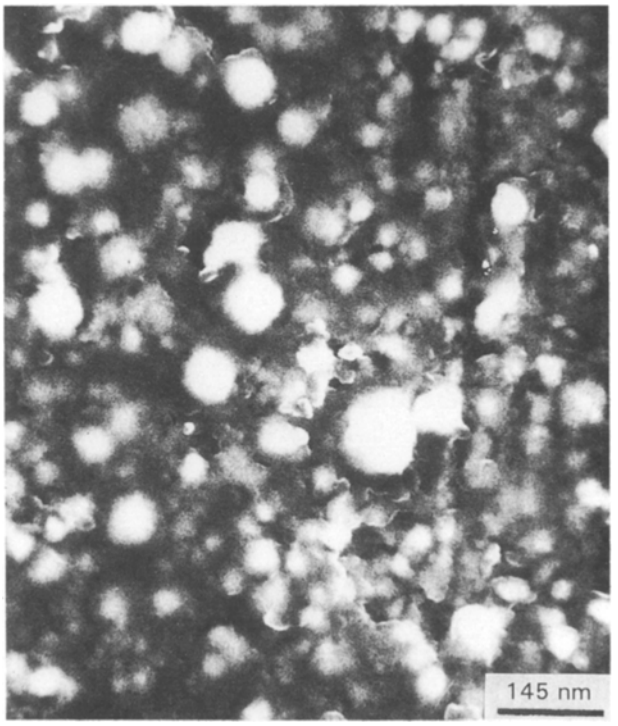

Figure 3 Scanning electron micrograph of a $Pd_{77.5}Au_6Si_{16.5}$ droplet with the diameter $D = 180$ μm.

4. Theoretical analysis of nucleation and phase formation

The description of the solidification behaviour of undercooled droplets requires knowledge of the driving force for phase formation, G_v, the activation energy for nucleation, G^*, the nucleation frequency, I_{ss}, and the crystal growth velocity, V.

4.1. The free-energy difference between solid and liquid

The free-energy difference, ΔG_v, can be written as [6]

$$\Delta G_v = \Delta S_f (T_L - T) - \frac{\Delta S_f (T_L - T)}{l_n (T_L/T_0)} + \frac{T \Delta S_f l_n (T_L/T)}{l_n (T_L/T_0)} \quad (2)$$

where, $\Delta S_f = \Delta H_f / T_L$ is the entropy of fusion, ΔH_f the heat fusion and T_0 the glassy transition temperature. Supposing an ideal glass transition temperature of $T_0 = 645$ K [7] and using the values for ΔH_f and the

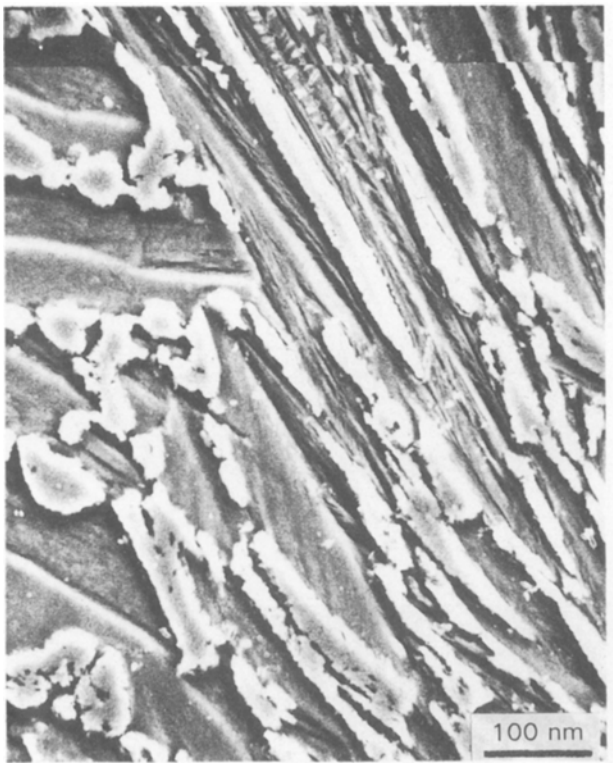

Figure 4 Scanning electron micrograph of the surface region of a $Pd_{77.5}Au_6Si_{16.5}$ droplet with diameter $D = 1000$ μm.

liquid temperature, T_L, of the various phases as given in Table I, the free-energy differences, ΔG_v (T), are calculated for the palladium solid-solution phase and Pd_3Si phase; the results are shown in Fig. 6a. For both phases, ΔG_v decreases monotonically with increasing temperature, T.

4.2. Activation energy for nucleation

According to classical nucleation theory, the activation threshold, ΔG^*, for the formation of spherical critical nuclei is given by [9]

$$\Delta G^* = \frac{16\pi}{3}\frac{\sigma^3}{\Delta G_v^2} f(\theta) \quad (3)$$

where σ is the interfacial energy of the solid–liquid interface, and $f(\theta)$ is the catalytic potency factor for heterogeneous nucleation which depends on the wetting angle, θ. We approximate σ by $\sigma_m T/T_m$ as proposed by Spaepen and Meyer [10] under the assumption that σ is entirely of entropic origin; here σ_m is a constant. For Pd_3Si, $\frac{16}{3}\pi\sigma^3 f(\theta) = 10^{-13} T^3/T_m^3$; this expression comes from the assumption that the activation energy, ΔG^*, for forming the critical nucleus is 65 kT at $\Delta T_r = T_m - T/T_m = 0.2$. Onorato and Uhlmann [11] have found that the difficulty in forming glasses is generally overestimated by using this nucleation barrier. They found reasonable agreement between calculations and experiment, for materials with cooling rates up to 300 Ks^{-1}, using values of 55–65 kT at $\Delta T_r = 0.2$ for ΔG^* [11].

The parameter is not accessible for direct measurements; in order to calculate the activation threshold, ΔG^*, of palladium solid-solution phase, we refer to a

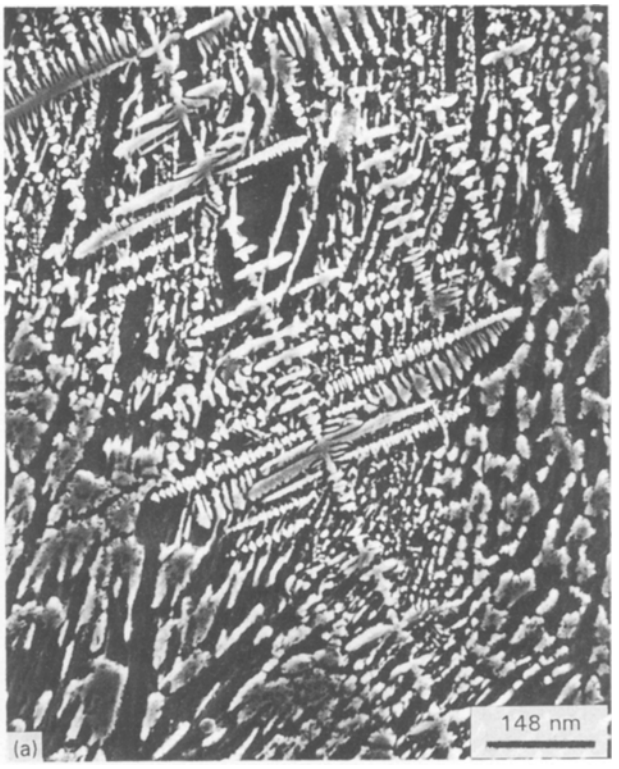

Figure 5 Scanning electron micrographs of the central region of a $Pd_{77.5}Au_6Si_{16.5}$ droplet with diameter $D = 1000$ μm: (a) unbranched dentritic growth of Pd_3Si; (b) branched triangular dentritic growth of Pd_3Si.

TABLE I Characteristic thermodynamic data for the calculation of the transformation behaviour of the undercooling melt into palladium solid-solution and Pd_3Si phase

	Palladium phase	Pd_3Si phase
Liquid temperature (K)	1033	1343
Heat fusion (J cm^{-3})	837 [7]	1680 [8]

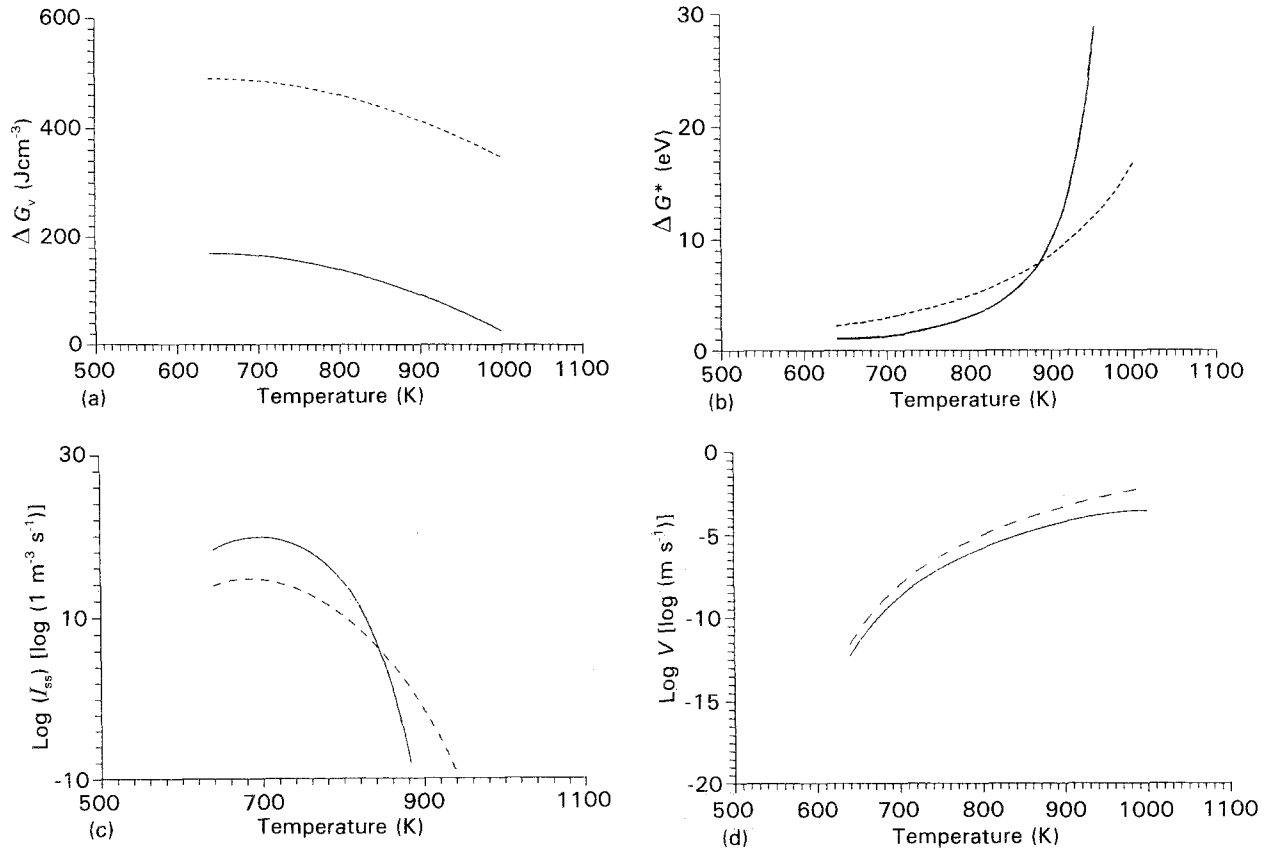

Figure 6 Temperature dependence of (a) the difference of free energy, (b) the activation energy for the formation of post-critical nuclei, (c) the nucleation frequency and (d) the crystal growth rate, as calculated for palladium solid-solution phase and Pd_3Si phase.(——) Palladium solid-solution, (– – –) Pd_3Si phase.

negentropic model as developed by Spaepen to estimate the interfacial energy [12]

$$\sigma = \alpha \frac{\Delta S_f T}{(N_L V_m^2)^{1/3}} \quad (4)$$

where α is a factor depending on the structure of the nucleus, N_L is Avogadro's number and V_m is the molar volume. The negentropic model gives $a = 0.86$ for f c c structure, hence a suitable value for palladium solid-solution phase.

In our experiment, EDS analysis show no other impurities in the droplets as would be expected for heterogeneous nucleation, and drop-tube processing eliminates container-wall-induced nucleation, so homogeneous nucleation for the formation of palladium solid-solution phase is supposed. Using the results of Fig. 6a, the temperature dependence of ΔG^* is calculated; the results are shown in Fig. 6b. From these results, the heterogeneous nucleation of Pd_3Si is seen to occur preferentially in the temperature range $T_L > T > 890$ K, and the homogeneous nucleation of the palladium solid-solution phase occurs mainly in the region $T < 890$ K. Calculation of the activation energies for nucleation gives the basis for the estimation of the nucleation rates.

4.3. Nucleation frequency

According to the kinetics of nucleation, the steady nucleation rate, I_{ss}, is given by [13]

$$I_{ss} = \frac{K_B T N_L}{3\eta(T)\, a_0^3} \exp(-\Delta G^*/K_B T) \quad (5)$$

where a_0 is a typical interatomic spacing and $\eta(T)$ represents the viscosity of the undercooled liquid. We use an expression for temperature-dependent viscosity proposed by Van den Beukel and Radelar [14]

$$\eta(T) = \eta_0 \exp \frac{B}{T - T_c} \exp(Q_n/K_B T) \quad (6)$$

where Q_n is the activation energy for viscous flow, and n, B, T_c the constants. Here $Q_n = 1.25$ eV, $n = 2.64 \times 10^{-7}$ P, $B = 1984$ K and $T_c = 529$ K. Fig. 6c shows the nucleation rate as a function of temperature for various phases.

4.4. Crystal growth velocity

The crystal growth velocity, V, is determined using the expression for diffusion-controlled growth of a planar rough interface [9]

$$V = \frac{D}{a_0}[1 - \exp(-\Delta G_v/RT)] \quad (7)$$

where D is the diffusion coefficient which is correlated to the viscosity via the Einstein–Stokes relation $D = K_B T/3\eta a_0$. Taking into account the results in Fig. 6a, the crystal growth velocity, V, has been calculated and the results are shown in Fig. 6d.

4.5. Time–temperature–transformation diagram

The Time–temperature–transformation (TTT) curves were calculated for the two phases considered here, on

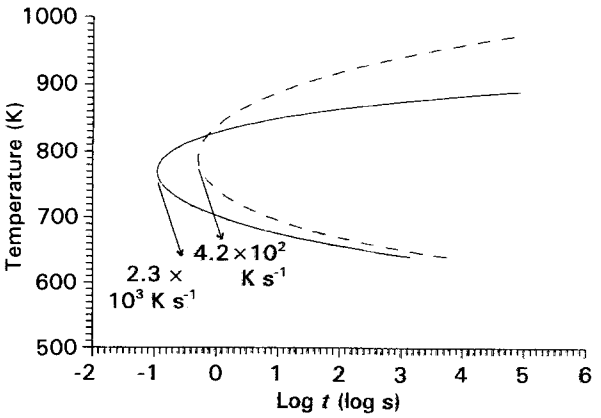

Figure 7 Time–temperature-transformation diagrams for palladium solid-solution phase and Pd_3Si phase.

the basis of nucleation and crystal growth behaviour discussed above. The time, t, necessary to produce a barely detectable fraction, $x = 10^{-6}$, of crystalline phase is given by [11]

$$X = \frac{\pi}{3} I_{ss} V^3 t^4 \tag{8}$$

Fig. 7 summarizes the TTT diagrams for Pd_3Si phase and palladium solid-solution phase. The TTT curves predict a sequence of phase formation during cooling. At a low cooling rate, Pd_3Si phase preferably crystallizes; however, at a cooling rate faster than the critical cooling rate of 4.2×10^2, Pd_3Si phase cannot occur and only palladium solid-solution is favoured. This sequence was actually observed in the experiments in Section 3, thus our calculation agrees with the undercooling experiment quite well. The complete avoidance of nucleation of the crystal phase would require a cooling rate larger than 2.3×10^3. In our experiment for the smallest droplets ($D = 180\ \mu m$), the cooling rate is only 1.5×10^3, this explains why we did not obtain a wholly amorphous structure.

5. Conclusions

Droplets of $Pd_{77.5}Au_6Si_{16.5}$ undergoing containerless processing in a 20 m drop tube can exhibit microstructures far from equilibrium. The microstructure strongly depends on droplet diameter. In small droplets ($D < 400\ \mu m$), only fine particles of palladium solid-solution phase were preferentially formed; in larger droplets Pd_3Si intermetallic phase appeared with dendritic growth. The nucleation and phase formation have been analysed within the nucleation and transformation theory. The results of the calculations were found to describe the experimentally observed undercooling and formation of palladium solid-solution phase and Pd_3Si compound phase.

References

1. LEWIS L. LACY, *J. Crystal Growth* **51** (1981) 47.
2. H. S. CHEN and C. E. MILLER, *Rev. Sci. Instrum.* **41** (1970) 1237.
3. D. M. HERLACH and F. GLLESSEN, *J. Phys. F Met. Phys.* **17** (1987) 1635.
4. F. GILLESSEN, *J. Less-Common Met.* **145** (1988) 145.
5. R. J. BAYUZICK, *Adv. Space Rev.* **4** (1984) 85.
6. F. GILLESSEN, *Mater. Sci. Eng.* **A134** (1991) 1221.
7. H. S. CHEN, *J. Appl. Phys.* **43** (1972) 1642.
8. KUNIMASA TAKESHITA, *Trans. Jpn. Met.* **24** (1983) 293.
9. J. W. CHRITIAN, "The Theory of Transformations in Metals and Alloys" (Pergamon, Oxford, 1975).
10. F. SPAEPEN and R. B. MEYER, *Scripta. Metall.* **34** (1976) 2129.
11. P. I. K. ONORATO and D. R. UHLMANN, *J. Non-Cryst. Solids* **22** (1976) 367.
12. F. SPAEPEN, *Acta Metall.* **23** (1975) 729.
13. D. TURNBULL, *Contemp. Phys.* **10** (1969) 473.
14. VAN DEN BEUKEL and RADELARS, *Acta Metall.* **31** (1983) 419.

Received 17 March 1992
and accepted 24 February 1993